Electrical Power and Energy Systems 109 (2019) 395–402

Contents lists available at ScienceDirect

Electrical Power and Energy Systems

journal homepage: www.elsevier.com/locate/ijepes

On-line partial discharge monitoring system for underground MV cables – Part II: Detection and location

Apostolos Milioudis[a,*], Georgios Andreou[b], Dimitris Labridis[b]

[a] Development and Operation Sector, Hellenic Distribution Network Operator (HEDNO S.A.), Thessaloniki, Greece
[b] Department of Electrical and Computer Engineering, Power Systems Laboratory (PSL), Aristotle University of Thessaloniki (AUTH), P.O. Box 486, 54124, Greece

ARTICLE INFO

Keywords:
Partial discharges (PDs)
Condition based maintenance
Electromagnetic transients modelling
Insulation degradation

ABSTRACT

Condition based maintenance constitutes a useful tool towards upgrading aging infrastructure in the context of asset management in smart grids. Towards that aim, on-line partial discharge (PD-OL) monitoring systems can provide useful information regarding insulation degradation, that can be used to prevent destructive faults. In this study, a set of novel algorithms is proposed for utilization in such a system. More specifically, an enhanced approach is proposed to denoise partial discharge (PD) associated measurements, by the utilization of the discrete wavelet transform (DWT). Moreover, an overall process is presented for the efficient detection of peaks in denoised signals, and the respective calculation of the PD apparent charge. Furthermore, algorithms are proposed for the detection and location of PDs in practical applications, taking also into account possible pulse reflections, and disregarding the corresponding false positive detections. All proposed methods are rigorously tested, and the respective results are presented.

1. Introduction

Underground networks constitute the backbone of urban medium voltage (MV) power distribution, covering vast areas and delivering large amounts of energy. The uninterrupted operation of underground distribution networks is of crucial importance for the overall system reliability. One of the major problems that may affect the network uninterrupted operation is the occurrence of partial discharges (PDs) on underground MV cables, which can lead to gradual insulation degradation, and finally to destructive faults.

The detection and location of PD activity can provide crucial information to the respective utility regarding the insulation condition of operating MV distribution cables [1–3] and MV equipment in general [4,5]. This can be achieved by the installation of on-line PD (PD-OL) monitoring systems, which can detect and locate PDs. The information related to the progression of the phenomenon over time can prevent the occurrence of destructive faults [6–8], hence improving system reliability indices, and preventing short circuit current stressing of other equipment. Hence, such a system can contribute towards one of the important aspects of smart grid that is to make the best use of existing assets by the implementation of optimized preventive maintenance [9–11] and intelligent asset condition awareness [12,13].

Detection of PD sources is a subject that has attracted intense research activity for a long time. Approaches using pattern recognition techniques have been proposed in the literature [14–16]. Other studies have focused on the modelling of PDs, taking into account the physics of the occurring discharges [17,18]. For practical applications such as PD-OL monitoring systems, the discharge can be considered as an impulse current of certain magnitude according to the respective charge [19–22]. In regard to the location of PD activity, systems have been proposed based on single end measurements, which utilize time domain reflectometry (TDR) along with signal processing techniques [23–25]. However, such systems can mainly be used off-line, and exhibit strict limitations regarding their efficiency and application scope [19].

One major advantage of an on-line system is the capability to operate under real operational conditions, hence eliminating the need to disconnect system components. Furthermore, the utilization of measurements at both ends of a monitored cable provides supplementary information regarding the location and apparent charge of the detected PD activity. Naturally, time synchronization of the respective measurements is of crucial importance. This can be achieved by the injection of a specific signal on the monitored cable, utilizing the known propagation time between the two cable ends, as described in [26].

However, PD-OL monitoring systems may have to operate under excessive noise conditions, therefore the utilization of a highly efficient denoising scheme is really important. The objective of a denoising process is to remove noise from the measured data as effectively as possible, while preserving the signal features which are essential for the

* Corresponding author.
E-mail address: A.Milioudis@deddie.gr (A. Milioudis).

https://doi.org/10.1016/j.ijepes.2019.02.018
Received 5 November 2018; Received in revised form 29 January 2019; Accepted 11 February 2019

detection and location of the PDs. Two main approaches have been proposed towards this purpose in the literature, i.e. the utilization of discrete wavelet transform (DWT) [27–31], and matched filter banks (MFB) [32,33]. These approaches share the main concept of comparing the PD associated signals to specific signal templates, while the denoising process is relied on the resemblance between them. Regarding the DWT approach, Ma et al. propose to base the selection of an optimal mother wavelet on the maximization of the cross correlation coefficient among PD associated pulses and wavelet families [27]. Zhou et al. suggest respectively that the optimal mother wavelet can be determined according to the energy distribution at different levels of decomposition [28]. Both methods have advantages and are able of providing efficient results. Additionally, Zhang et al. have suggested that the determination of the thresholds for different levels of decomposition can come from the knowledge of the existing noise levels [29,30].

In this manuscript, a novel denoising process in suggested, utilizing DWT and incorporating the advantages of already existing methods in the literature [27,28]. Moreover, a peak detection process is proposed that can be implemented in practical applications, along with a respective process that can efficiently determine the apparent charge of detected and located PD activity. Furthermore, two algorithms are proposed for the detection and location of PDs. The second algorithm differs from the first one in its ability to account for pulse reflections, being thus able to disregard false positive detections associated with reflections instead of first arriving pulses. All proposed methods are rigorously tested, and the respective results validate their efficiency.

2. Proposed denoising process

Typically, the measured signals associated with PD activity are distorted with significant noise levels, therefore the denoising process is of crucial importance. Two main methods have been proposed in the literature focusing on the implementation of discrete wavelet transform (DWT), and specifically on the mother wavelet selection procedure. The first one, suggested by Ma et al. [27], aims at the maximization of the cross correlation coefficient relating the PD associated pulses, denoted as vector $\mathbf{X}$, and the mother wavelet data vocabulary $\mathbf{V}$, with entries denoted as $\mathbf{Y}$, as

$$\arg\max_{\forall \mathbf{Y}\in\mathbf{V}} \frac{\sum_{i=1}^{K}(X_i-\overline{X})(Y_i-\overline{Y})}{\sqrt{\sum_{i=1}^{K}(X_i-\overline{X})^2\cdot\sum_{i=1}^{K}(Y_i-\overline{Y})^2}} \tag{1}$$

where K is the number of available samples corresponding to vectors $\mathbf{X}$ and $\mathbf{Y}$ and notation $\overline{(\cdot)}$ corresponds to the mean value of the involved vector.

A second approach relies on the energy distribution of the DWT coefficients at different levels of decomposition. The most suitable mother wavelet is selected, so that the corresponding energy distribution is concentrated at specific levels of decomposition and does not spread significantly over various levels. This can result into better denoising, hence the PD signal could be recovered more easily [28]. Threshold selection is conducted for both cases by hard thresholding, with the threshold being computed for each level.

A new methodology is proposed in this work, aiming at taking advantage of both aforementioned techniques. This is achieved by adopting the selection of the mother wavelet of the first approach [27], incorporating at the same time the adaptive thresholding technique of the second approach [28]. More concretely, the levels of decomposition with insignificant energy distribution, i.e. smaller than an energy threshold ε_{en}, are not taken into account, by raising the respective threshold at a value larger than the maximum coefficient at the specific level. At the same time, the thresholds for levels with significant energy distribution are computed as in [27,28]. The proposed adaptive thresholding approach is mathematically formulated as

$$\lambda_j = \begin{cases} \left|\frac{m_j}{0.6745}\cdot\sqrt{2\cdot\log(n_j)}\right| & \text{if } \frac{\sum_{i=1}^{N_k}(Cd_{ji})^2}{\sum_{j=1}^{N_d}\sum_{i=1}^{N_k}(Cd_{ji})^2} > \varepsilon_{en} \\ 1.5\cdot\max(|Cd_j|) & \text{elsewhere} \end{cases} \tag{2}$$

where m_j is the median value of the coefficients at level j, Cd_{ji} is the i_{th} coefficient at level j of total N_k number of coefficients at this particular level, n_j is the number of coefficients at level j and N_d the total number of decomposition levels.

In conclusion, the proposed method uses the mother wavelet selection procedure as it is described in [27]. At the same time, it exploits the advantages of mother wavelet selection procedure presented in [28], by incorporating a novel adaptive thresholding process that is presented in Eq. (2), which takes into account the energy distribution at each decomposition level.

3. PD detection and location in practical applications

The utilization of synchronized measurements at both monitored cable ends provides the ability of both detecting and locating PD sources, as long as an efficient algorithm is implemented. The outputs of such an algorithm correspond to the location of a PD source, along with the respective apparent charge of the detected discharge. Therefore, apart from the defected cable parts that can be located, the progress of the phenomenon in time can also be monitored focusing on the apparent charge variation of the occurring discharges.

Let us consider that the denoised voltages corresponding to measurements at both monitored cable ends, k an m, are $u_k^*(t)$ and $u_m^*(t)$, respectively. These denoised measurements contain PD associated pulses at specific time instances, corresponding to the arrival times at each cable end. Assuming that the detected pulses are generated by a PD located at some point along the monitored cable, they will arrive at cable end k at time instant t_{oa_k}, and at cable end m at time instant t_{oa_m}. The difference in time of arrival, Δt_{oa}, is defined as

$$\Delta t_{oa} = t_{oa_m} - t_{oa_k}. \tag{3}$$

Considering that the monitored cable segment has a length of l_c, and the traveling time from one cable end to the other is t_c, the location of the occurring PD with respect to cable end k, z_{PD}, can be computed as

$$z_{PD} = \frac{t_c - \Delta t_{oa}}{2\cdot t_c}\cdot l_c. \tag{4}$$

In practice, the effectiveness of the PD location algorithms relies heavily on three important aspects. The first aspect corresponds to the necessity that the times of arrivals taken into account in (3) are associated with the same PD activity. The second aspect deals with the fact that these arrival times correspond to first arriving pulses and not to their reflections. The inability of a PD location algorithm to account for these two issues can significantly deteriorate its respective performance. Finally, the third and crucial aspect is associated with the correct calculation of the apparent charge corresponding to the PD activity from both cable ends. In order to address all these three aspects, robust approaches of peak detection, apparent charge calculation, detection and location algorithms have to be implemented.

3.1. Peak detection process

In order to address the first important aspect, let us assume that two vectors are available after the denoising process of the sampled measured signals at both cable ends k and m, i.e. $\mathbf{u_k^*}$ and $\mathbf{u_m^*}$ respectively. By applying a peak detection algorithm, the occurring peaks and their respective time instances can be extracted from the vectors of measurements. Peaks cannot be obtained by comparing the sample values, instead the first order difference can be used to identify them [34]. Specifically, a peak occurs when the trend of the first order difference changes from positive to negative. Apart from that, the results of the peak detection algorithm can be enhanced by introducing a minimum

amplitude for the detected peaks, ε_p, associated to the minimum detected charge of a PD regarding the system under design. Furthermore, the introduction of a minimum time difference among successive detected peaks, ε_t, is important. The measured PD associated pulses can exhibit several peaks due to their fluctuating shapes, hence in order to avoid detecting secondary peaks in a PD associated pulse, ε_t has to be utilized. Naturally, the value of ε_t has to be equal to the expected time duration of a PD associated pulse. The outputs of the simple peak detection process are vectors containing the values of the detected peaks for each measured cable end, namely $\mathbf{p_k}$ and $\mathbf{p_m}$, for cable end k and m respectively. Moreover, the time stamps corresponding to the detected peaks form two more vectors, $\mathbf{T_{oa_k}}$ and $\mathbf{T_{oa_m}}$ respectively. Focusing on the peak amplitude introduced limitation, let us assume that the i_{th} element of vector $\mathbf{p_k}$ corresponds to a peak amplitude equal to x, detected at cable end k. It is necessary that this peak satisfies the minimum amplitude condition as it is expressed in

$$p_k(i) = x, \quad x > \varepsilon_p, \tag{5}$$

while the same expression can be easily appropriately modified for peaks detected in measurements coming from cable end m.

Furthermore, the time difference among successive elements of vectors $\mathbf{T_{oa_k}}$ and $\mathbf{T_{oa_m}}$ has to be larger than the expected duration of a PD associated pulse. For that reason, considering the difference, δ, among two successive elements of $\mathbf{T_{oa_k}}$, i.e. $T_{oa_k}(i)$ and $T_{oa_k}(i+1)$, the following criterion has to be met

$$T_{oa_k}(i+1) - T_{oa_k}(i) = \delta, \quad \delta > \varepsilon_t, \tag{6}$$

while the same formulation can easily be expressed for measurements coming from cable end m.

3.2. Apparent charge calculation

An efficient PD detection and location procedure is also based on the accurate apparent charge calculation corresponding to the PD activity at both cable ends. Let us consider a PD occurring at distance equal to z_{PD} from cable end k. The PD current can be represented in the time domain with a vector $\mathbf{I^t_{PD}}$ consisted of N time sample elements as

$$\mathbf{I^t_{PD}} = [1 \quad 0 \quad \cdots \quad 0]. \tag{7}$$

The first arriving current pulse caused by the studied PD and measured at cable end k forms in the frequency domain a vector denoted as $\mathbf{I^f_k}$. The n_{th} element of this vector is computed as in

$$I^f_k(n) = \tau_k(n) \cdot e^{-\gamma(n) \cdot z_{PD}} \cdot I^f_{PD}(n) \tag{8}$$

where $\tau_k(n)$ is the transmission coefficient at cable end k corresponding to the n_{th} examined frequency, $\gamma(n)$ the propagation constant at the same frequency, and $I^f_{PD}(n)$ is the n_{th} element of vector $\mathbf{I^f_{PD}}$, which is the frequency domain equivalent of PD current $\mathbf{I^t_{PD}}$. In time domain the first arriving pulse can be computed by applying an inverse Fourier transform (IFFT), and the outcome can be used as a template pulse $\mathbf{I^{tem}_k}$ corresponding to the specific location of occurrence. Considering the n_{th} peak detected at cable end k, $p_k(n)$, the template pulse can be normalized in order for its maximum value to be equal to this detected peak as in

$$\mathbf{I^{norm}_k} = \mathbf{I^{tem}_k} \cdot \frac{p_k(n)}{\max(\mathbf{I^{tem}_k})} \tag{9}$$

where notation $\max(\cdot)$ denotes the maximum value of the enclosed expression.

The normalized template pulse can be used in order to calculate the apparent charge of the PD as shown in the following equation

$$Q_k = 2 \cdot max\left\{ \left| IFFT\left[\frac{FFT(\mathbf{I^{norm}_k})}{e^{-\gamma \cdot z_{PD}} \cdot \tau_\mathbf{k}} \right] \right| \right\} \cdot dt \tag{10}$$

where the notations $FFT(\cdot)$ and $IFFT(\cdot)$ denote the fast Fourier transform (FFT) and the inverse FFT of the enclosed vectors, and dt is the sampling time. It is shown that the apparent charge is computed as the product of the maximum absolute value of the current corresponding to the PD, i.e. the expression inside the brackets, and the sampling time. Naturally, the same process may be used in order to calculate the apparent charge as measured from cable end m, simply by adjusting the involved values accordingly.

The proposed methodology for the calculation of a PD apparent charge has the advantage that it requires only the location of the PD, and the respective detected peak, as obtained after the denoising and peak detection processes. Therefore, it can perform efficiently regardless of the effectiveness of the denoising process. Furthermore, it comprises an important part of the overall detection and location process, as it is used in combination with measurements from both cable ends to determine a valid PD detection and location, as explained in the next subsection.

3.3. Detection and location neglecting pulse reflections

After the peak detection process for every element of vector $\mathbf{T_{oa_k}}$, a process has to be implemented to determine possible arriving times in $\mathbf{T_{oa_m}}$ that could correspond to the same PD activity. For that reason, the search area regarding the arrival times at cable end m is reduced to the set of values $[t_{down}, t_{up}]$ which are equal to $[T_{oa_k}(i) - t_c, T_{oa_k}(i) + t_c]$ respectively. The reason behind this selection is the physical time limit imposed by the cable propagation time for the extraction of plausible arriving time pairs. Consequently, for every element of vector $\mathbf{T_{oa_k}}$, two corresponding vectors can be formed. The first one, denoted as $\mathbf{T^{cand}_{oa_m}}$, contains pulse arriving times detected at cable end m within the computed search area $[t_{down}, t_{up}]$, while the second one, denoted as $\mathbf{p^{cand}_m}$, contains the respective detected peak values. Subsequently, for every element in vector $\mathbf{T^{cand}_{oa_m}}$ the respective PD location, z^{cand}_{PD}, can be computed. If the computed respective apparent charges Q_k and Q_m have sufficiently similar values, as determined by a convergence criterion ε_c, the algorithm is considered to have detected and located a PD. The overall procedure is also included in Algorithm 1.

Algorithm 1. PD detection and location algorithm

1: Acquire measurement vectors $\mathbf{u_k}$ and $\mathbf{u_m}$.
2: Acquire vectors $\mathbf{u^*_k}$ and $\mathbf{u^*_m}$ from denoising procedure.
3: Apply peak detection to denoised vectors and acquire vectors $\mathbf{p_k}$, $\mathbf{p_m}$, $\mathbf{T_{oa_k}}$ and $\mathbf{T_{oa_m}}$ taking into account limitations as stated in Eqs. (5) and (6).
4: $N \leftarrow$ number of elements of $\mathbf{T_{oa_k}}$.
5: **for** $i = 1$ to N **do**
6: $t_{up} \leftarrow T_{oa_k}(i) + t_c$
7: $t_{down} \leftarrow T_{oa_k}(i) - t_c$
8: Reduce the search domain into $[t_{down}, t_{up}]$.
9: Acquire the elements of $\mathbf{T_{oa_m}}$ that belong into the set of values $[t_{down}, t_{up}]$ and their respective peak values from $\mathbf{p_m}$.
10: Form vectors $\mathbf{T^{cand}_{oa_m}}$ and $\mathbf{p^{cand}_m}$ using the values from previous step.
11: $M \leftarrow$ number of elements of $\mathbf{T^{cand}_{oa_m}}$.
12: **for** $j = 1$ to M **do**
13: $\Delta t \leftarrow T^{cand}_{oa_m}(j) - T_{oa_k}(i)$
14: $z^{cand}_{PD} \leftarrow \frac{t_c - \Delta t}{2 \cdot t_c} \cdot l_c$
15: Calculate corresponding apparent charges of discharges for both cable ends, Q_k and Q_m.
16: **if** $\left| \frac{Q_k - Q_m}{Q_m} \right| \leqslant \varepsilon_c$ **do**
17: Store location and apparent charge for detected PD.
18: **end if**
19: **end for**
20: **end for**

3.4. Detection and location taking into account possible pulse reflections

The approach presented in Section 3.3 is capable of associating pulses detected at both cable ends which correspond to the same PD activity, by comparing the respective apparent charge of every pair of detected pulses, as shown in Algorithm 1.

However, despite the fact that this approach may be effective for many cases, it cannot account for pulse reflections. These become significant, and have to be taken into consideration, in cases where the attenuation introduced by the monitored cable is not significant, as well as in cases of certain values of signal to noise ratio (SNR) exhibited at monitored cable ends. Neglecting pulse reflections in such cases can result in false positive detection of PD activity, since the reflected pulses will be detected and associated to different PD activity than the one corresponding to the first arriving pulses. For that reason, the algorithm presented in the previous subsection has to be appropriately modified.

In order to avoid false positive PD detection due to reflections, let us consider that a PD has been detected and located correctly. Thus, the detected and associated pulses correspond to the first arriving pulses at both cable ends, regarding a PD located at some point along the length of the monitored cable. Let us assume that the detected pulses correspond to time instances t_k^{PD} and t_m^{PD} of measurements from cable end k and m, respectively, regarding a detected PD at location z_{PD}. The time instances at which the reflected pulses will arrive at both cable ends can easily be computed, as the monitored cable length and the propagation time between both cable ends are known. Therefore, for every detected PD the expected time instances corresponding to reflections can be calculated and excluded from the procedure as restricted ones. For that reason, a vector containing restricted time instances with respect to every detected pulse at cable end k, $\mathbf{RL_k}$, is introduced, corresponding to reflections. Similarly, vector $\mathbf{RL_m}$ formed by restricted time instances for cable end m is also introduced. The number of respective elements for both vectors can be limited to N significant reflections, the n^{th} elements of which are calculated as

$$RL_k(n) = \begin{cases} 2\cdot(n-1)\cdot t_c & n \in O \\ [l_c - 2z_{PD} + (n-1)\cdot l_c]\cdot\frac{t_c}{l_c} & n \in E \end{cases} \tag{11}$$

$$RL_m(n) = \begin{cases} 2\cdot(n-1)\cdot t_c & n \in O \\ [2z_{PD} + (n-2)\cdot l_c]\cdot\frac{t_c}{l_c} & n \in E \end{cases} \tag{12}$$

where set E corresponds to the positive, non-zero even numbers, $E = \{2k: k \in \mathbb{N}^+\}$, while set O corresponds to the positive, non-zero odd numbers, $O = \{(2k-1): k \in \mathbb{N}^+\}$.

Consequently, a set of vectors can be formed for every detected PD, containing time instances corresponding to reflections, in order for them to be disregarded in the remaining detection and location procedure. Therefore, vectors $\mathbf{RT_k}$ and $\mathbf{RT_m}$ can be formed for every detected first PD pulse arriving at cable ends k and m at time instances t_k^{PD} and t_m^{PD}, respectively. The aforementioned vectors are calculated as

$$\mathbf{RT_k} = \mathbf{RL_k} + t_k^{PD} \tag{13}$$

$$\mathbf{RT_m} = \mathbf{RL_m} + t_m^{PD}. \tag{14}$$

Thus, for a new valid PD detection and location, the corresponding time instances have to be excluded from the vectors containing restricted time instances, $\mathbf{RT_k}$ and $\mathbf{RT_m}$.

The proposed approach is presented in Algorithm 2 in more detail. Naturally, there are significant differences in comparison with Algorithm 1, which does not account for possible reflection detection. In particular, the time instances corresponding to detected pulses at both cable ends are compared to the elements of vectors $\mathbf{RT_k}$ and $\mathbf{RT_m}$. If the minimum absolute value of the distance in time for both vectors is lower than a predefined convergence criterion denoted as ε_{rt}, the associated pulses are considered to correspond to the same PD activity, hence the location and the charge are stored as the PD activity is regarded as detected and located. For every valid PD detection, vectors $\mathbf{RT_k}$ and $\mathbf{RT_m}$ are updated respectively, by incorporating new computed elements. The new version of the vectors will be used in order to exclude possible pulse reflections, hence false positive detections, for following pairs of detected pulses at both cable ends.

Algorithm 2. PD detection and location algorithm taking into account reflections

1: Acquire measurement vectors $\mathbf{u_k}$ and $\mathbf{u_m}$.
2: Acquire vectors $\mathbf{u_k^*}$ and $\mathbf{u_m^*}$ from denoising procedure.
3: Apply peak detection to denoised vectors and acquire vectors $\mathbf{p_k}$, $\mathbf{p_m}$, $\mathbf{T_{oa_k}}$ and $\mathbf{T_{oa_m}}$ taking into account limitations as stated in Eqs. (5) and (6).
4: Initialize empty vectors $\mathbf{RT_k}$ and $\mathbf{RT_m}$.
5: $N \leftarrow$ number of elements of $\mathbf{T_{oa_k}}$.
6: **for** $i = 1$ to N **do**
7: $t_{up} \leftarrow T_{oa_k}(i) + t_c$
8: $t_{down} \leftarrow T_{oa_k}(i) - t_c$
9: Reduce the search domain into $[t_{down}, t_{up}]$.
10: Acquire the elements of $\mathbf{T_{oa_m}}$ that belong into the set of values $[t_{down}, t_{up}]$ and their respective peak values from $\mathbf{p_m}$.
11: Form vectors $\mathbf{T_{oa_m}^{cand}}$ and $\mathbf{p_m^{cand}}$ using the values from previous step.
12: $M \leftarrow$ number of elements of $\mathbf{T_{oa_m}^{cand}}$.
13: **for** $j = 1$ to M **do**
14: $\Delta t \leftarrow T_{oa_m}^{cand}(j) - T_{oa_k}(i)$
15: $z_{PD}^{cand} \leftarrow \frac{t_c - \Delta t}{2\cdot t_c}\cdot l_c$
16: Calculate corresponding apparent charges of discharges for both cable ends, Q_k and Q_m.
17: **if** $\left|\frac{Q_k - Q_m}{Q_m}\right| \leqslant \varepsilon_c$ **then**
18: $\mathbf{TD_k} \leftarrow T_{oa_k}(i) - \mathbf{RT_k}$
19: $\mathbf{TD_m} \leftarrow T_{oa_m}^{cand}(j) - \mathbf{RT_m}$
20: **if** $min(|TD_k|) < \varepsilon_{rt}$ and $min(|TD_m|) < \varepsilon_{rt}$ **then**
21: Store location and charge for detected PD.
22: Calculate $\mathbf{RL_k}$ $\mathbf{RL_m}$ using (11) and (12).
23: Calculate new elements for $\mathbf{RT_k}$ and $\mathbf{RT_m}$.
24: Update $\mathbf{RT_k}$ and $\mathbf{RT_m}$.
25: **end if**
26: **end if**
27: **end for**
28: **end for**

An overall overview of the overall process, including the two types of algorithms is presented in Fig. 1.

4. Simulations

The proposed approaches have to be tested in order to validate their ability to provide enhanced results as compared to already existing formulations. Bearing that in mind, several tests have to be conducted in order to evaluate all proposed techniques, i.e. the novel proposed denoising process which combines two different approaches existing in the literature, the peak detection algorithm, the apparent charge calculation process, as well as the two different versions of detecting and locating algorithms, with the second one being also able to account for pulse reflections.

The selected test case consists of the same cable configuration as in Part I of the manuscript. Hence, the monitored cable segment connects two RMUs, which are modelled as described in Part I and in [19].

First of all, the proposed enhanced denoising technique is put to the test. The method implements DWT with the mother wavelet being selected based on the maximization of the cross correlation coefficient among the expected PD signals and the wavelet candidates. After rigorous testing, the Daubechies 2 wavelet family [35], i.e. db2, was selected because it maximized the cross correlation coefficient. Apart from that, the proposed technique changes the way the thresholds are calculated for each decomposition level, in order to incorporate the

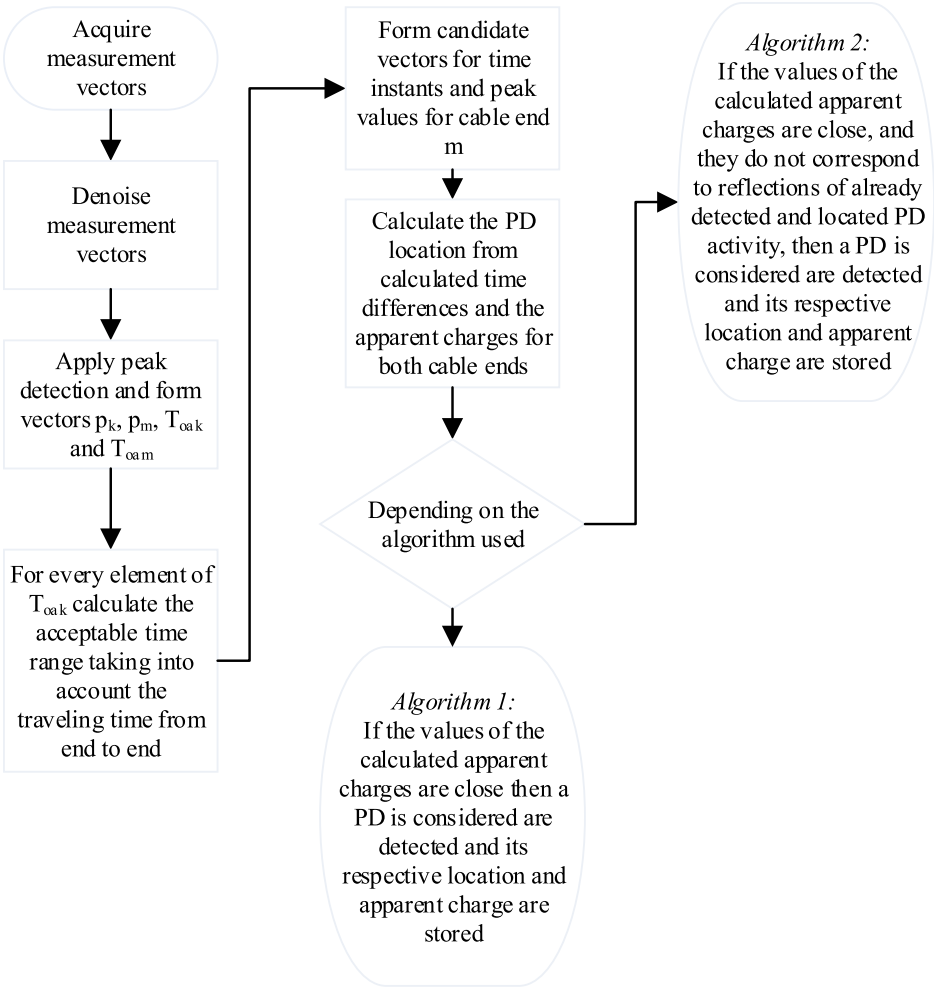

Fig. 1. Overview of the overall process.

advantages of the denoising methodology proposed in [28]. For that reason, the energy regarding the coefficients for several decomposition levels is plotted in Fig. 2. It is evident that the largest part of the energy is concentrated in decomposition level 4, and also that the energy of some levels is insignificant. Hence, by applying an energy threshold ε_{en}, as defined in (2), equal to 0.05, several levels will be disregarded, as this threshold exceeds their respective maximum coefficients.

The proposed denoising scheme is tested in comparison with

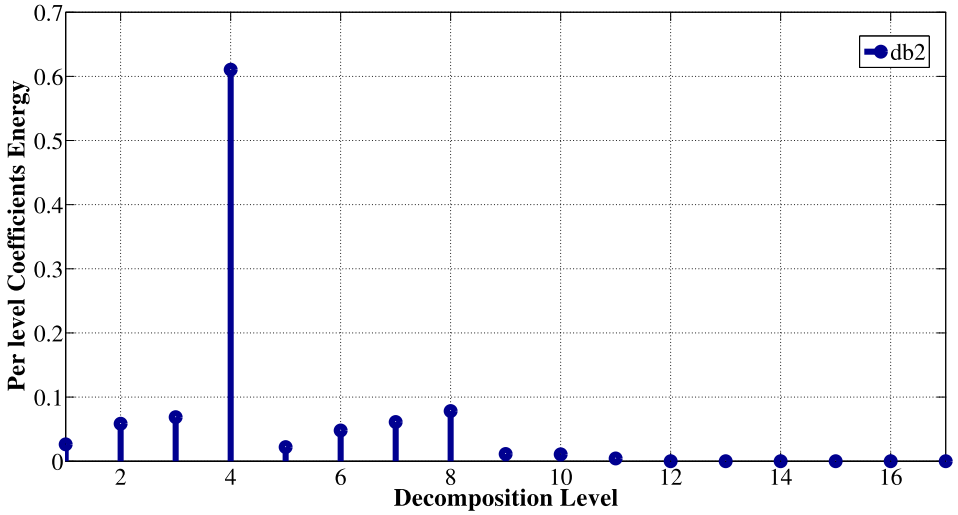

Fig. 2. Coefficients' energy per decomposition level using db2 wavelet family.

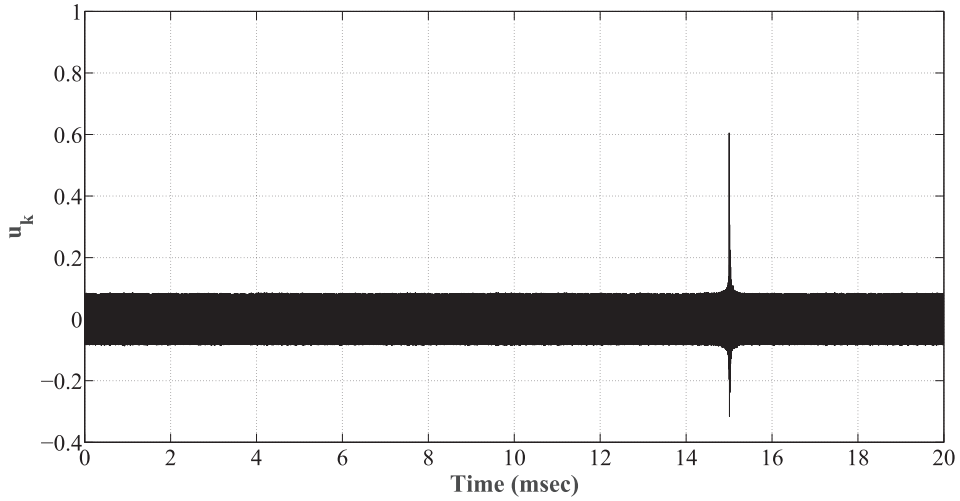

Fig. 3. Original noisy signal.

proposed approaches by Ma et al. [27] and Zhou et al. [28] for the noisy signal presented in Fig. 3 corresponding to −25 dB SNR, and the results are presented in Fig. 4. The denoised signal u_k^* corresponds to a case at which a PD occurs at 15 ms and 300 m away from cable end k. As shown in Fig. 4, all denoising schemes are able to effectively extract the pulses corresponding to the actual PD, which is also magnified in the plot. However, it is also evident that the two comparison methods also extract pulses that do not actually correspond to PD activity, as it is emphasized in the first two included magnified plots. This specific inefficiency can lead to undesired false positive detections, hence to deteriorated overall detection and location results.

Moreover, the overall performance of the denoising methods is tested for various cases of PD activity, as well as for different SNR scenarios. The selected performance metrics are the precision and recall of the denoising process [36,37]. Specifically, the denoising process is considered to provide true positive detection when a pulse corresponding to PD activity is present into the denoised signal. Moreover, false positive detections are considered when a noise pulse is present into the denoised signal, and false negative detections correspond to PD pulses that are absent from the denoised signal. Focusing on the content of Table 1, it is deduced that the proposed methodology produces enhanced results in comparison with the other two schemes for every tested SNR scenario, exhibiting significantly high values of precision and recall. The performance of all methods deteriorates for lower SNR values, as expected.

Table 1
Metrics of denoising methods.

	Ma et al.		Zhou et al.		Proposed	
SNR (dB)	Precision	Recall	Precision	Recall	Precision	Recall
−5	0.89	1.00	0.75	0.99	0.96	1.00
−15	0.83	1.00	0.74	0.98	0.85	1.00
−25	0.62	0.98	0.73	0.97	0.82	0.99
−35	0.17	0.90	0.52	0.90	0.75	0.95
−45	0.01	0.07	0.02	0.05	0.10	0.10

Furthermore, the testing results regarding the peak detection process are presented in Fig. 5, corresponding to the peaks detected in the denoised voltage signals u_k^*. Specific variables have to be set in this case, according to the PD associated pulse shapes and the minimum desired PD charge to be detected. More specifically, for the studied test case, the variable ε_p was set to 7 mV, which corresponds to the minimum detected PD charge of 0.5 nC, whereas variable ε_t was set to 2 μs in order to prevent several peak detections on the same PD associated pulse. Moreover, the SNR was set to −15 db, and the depicted

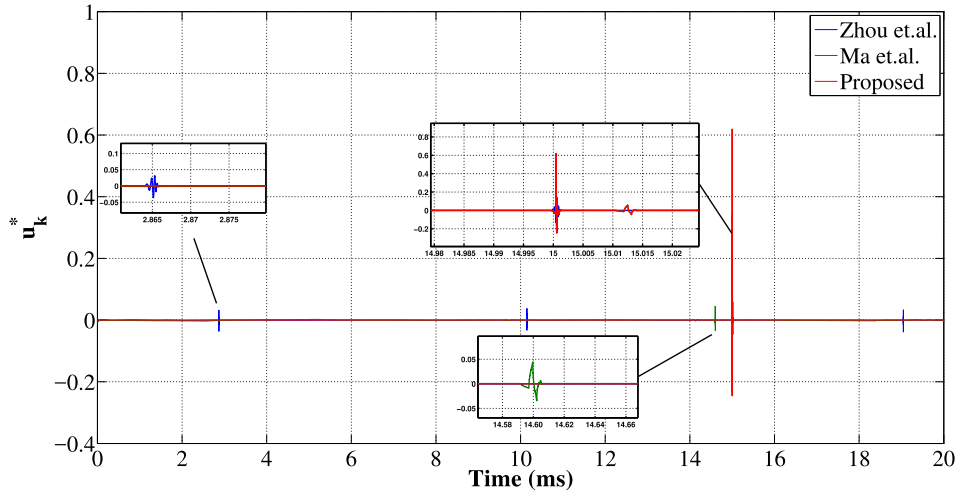

Fig. 4. Comparison of denoising schemes.

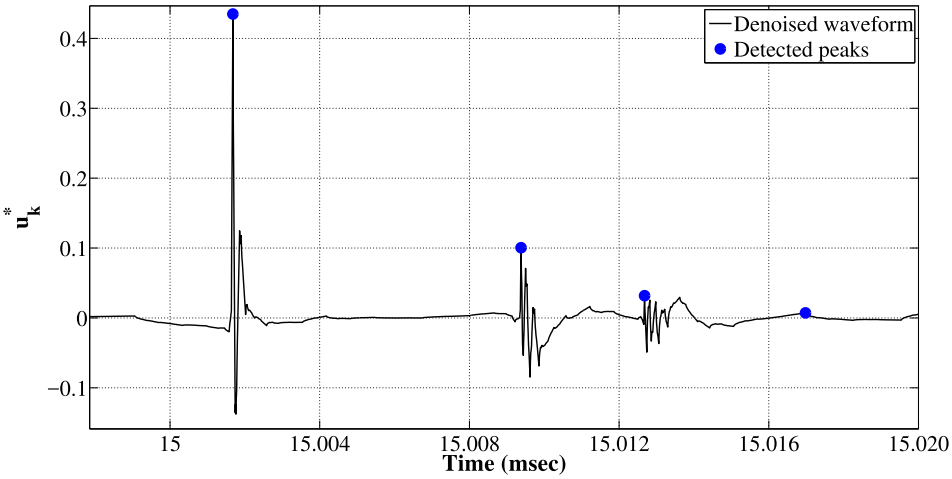

Fig. 5. Detected peaks on denoised signal from cable end *k*.

Table 2
Apparent charge detection.

SNR (dB)	Q_{app} (nC)	Q_{det} (nC)	Deviation (%)
−5	1	0.98	2
	6	5.84	3
−10	1	0.97	3
	6	5.84	3
−15	1	0.98	2
	6	5.84	3
−20	1	0.99	1
	6	5.67	5.4
−25	1	0.94	6
	6	5.55	7.4
−30	1	0.89	11
	6	5.54	7.6

PD corresponds to a 41 nC charge, located 300 m away from cable end *k*. The detected peaks are highlighted in the figures, illustrating that the proposed approach is able to provide as an outcome the actual points corresponding to the arriving pulses. Peak detection can be really tricky in signals containing several peaks, but the introduction of the minimum peak height and the time difference between peaks in the proposed approach is capable of providing correct results, as shown.

The next test case aims to evaluate the performance of the proposed scheme, as presented in Section 3.2, in regard to the ability to effectively detect the apparent charge of occurring PD activity. Towards that purpose, several scenarios were tested regarding various SNR cases, as presented in Table 2. It may be observed that the results are very good, exhibiting relatively small percentage deviation even for very low SNR values, and proving thus that the proposed approach is highly effective.

In the next test case, the overall detection and location procedures are evaluated as they were described in Sections 3.3 and 3.4. The first version, denoted as Algorithm 1, deals with the detection and location process neglecting the possible occurrence of pulse reflections, whereas Algorithm 2 also accounts for possible reflections, ensuring that the corresponding pulses will not lead to false positive PD detection. For the testing procedure, variable ε_c was set to 0.5, while the utilized noise levels corresponded to a SNR value equal to −15 db. The respective results for various test cases are presented in Table 3, and it is evident that both algorithms can detect effectively the location and the apparent charge of the occurring PDs. For every tested scenario, the precision was significantly improved. Evidently, false detections as expressed by the precision metric are much more when the reflections are not taken into account as in Algorithm 1. It is shown that the utilization of Algorithm 2 significantly improves the overall performance by not exhibiting false positive detections.

The final case presents the overall statistics of the proposed approach, as they were obtained by its application in a large number of scenarios. More specifically, for each SNR scenario, the method was implemented for all possible PD locations along the monitored cable, with a distance step equal to 5 m, and for apparent charges ranging from 1 to 20 nC, with a charge step equal to 0.5 nC. These variables set a large number of scenarios that were simulated. The results are included in Table 4 in terms of mean and median deviation regarding detected charge and location, as well as overall method precision. It may be seen that the overall performance is highly effective in both detecting the actual charge associated with PD activity, and locating the defect. The mean deviation in respect to apparent charge detection is for all noise level cases lower than 10%, whereas the deviation in the location is close to 0.5 m. This location error is considered to be relatively low in practical applications, at which the substitution of the defected part of the cable will require the on-site visit by a utility crew which can accurately spot the exact defect location. Furthermore, the overall precision is close to unity for each SNR scenario, showing that the overall detecting and locating capability is highly efficient.

5. Conclusion

The manuscript includes a set of approaches that can be used in PD-OL systems in order to effectively detect and locate PD activity along the length of the monitored cable towards the enhancement of the asset management in the smart grid context. Specifically, a novel denoising method implementing DWT is proposed. This approach combines the advantages of methods already existing in the literature, by appropriately selecting the mother wavelet family and the respective thresholds at different levels of decomposition according to the energy of the wavelet coefficient at each specific level. The method is tested and compared with already existing methods, and is proven to provide enhanced results by significantly improving the precision and recall of the denoising process. Moreover, a peak detection method is proposed, and is shown that it can provide the correct peaks in denoised PD associated signals that exhibit several peaks. The proposed approach can also effectively derive the apparent charge of the detected PD activity as indicated by the conducted tests. Moreover, two algorithms are presented which can provide the detection and location of PD activity, with the second one being able to also take into account possible pulse reflections, and avoid respective false positive detections. The two algorithms are tested and it is shown that the consideration of reflections

Table 3
Detection and location algorithms' comparison.

Discharge Data		Algorithm 1			Algorithm 2		
Location (m)	Q_{app} (nC)	Location (m)	Q_{det} (nC)	Precision	Location (m)	Q_{det} (nC)	Precision
90	21	90.85	21.42	0.33	90.85	21.42	1.00
150	26	150.86	26.37	0.25	150.86	26.37	1.00
30	76	30.84	76.13	0.33	30.84	76.13	1.00
660	11	660.02	11.53	0.50	660.02	11.53	1.00
950	21	950.84	21.75	0.50	950.84	21.75	1.00
700	56	700.02	57.04	1.00	700.02	57.04	1.00
650	91	650.89	92.40	0.25	650.89	92.40	1.00
330	51	330.02	55.02	1.00	330.02	55.02	1.00

Table 4
Overall method statistics.

	Detected charge		Location		
SNR (dB)	Mean Deviation (%)	Median Deviation (%)	Mean Deviation (m)	Median Deviation (m)	Precision
−5	4.57	5.98	0.39	0.02	0.99
−15	4.65	6.01	0.39	0.02	0.98
−25	6.12	6.95	0.46	0.03	0.97
−35	8.56	9.02	0.64	0.15	0.96

can lead to significantly enhanced results in terms of precision. Through the thorough testing procedure of the overall methodology, it is shown that PD activity is correctly detected in terms of apparent charge and located along the monitored cable.

Acknowledgments

The work of A.N. Milioudis is supported by the "IKY Fellowships of Excellence for Postgraduate Studies in Greece – Siemens Program."

References

[1] Zhu M-X, Wang Y-B, Chang D-G, Zhang G-J, Tong X, Ruan L. Quantitative comparison of partial discharge localization algorithms using time difference of arrival measurement in substation. Int J Electr Power Energy Syst 2019;104:10–20. https://doi.org/10.1016/j.ijepes.2018.06.036 http://www.sciencedirect.com/science/article/pii/S0142061518308275 .

[2] Hashmi M, Lehtonen M, Nordman M, Jabbar RA, Qureshi SA. Wavelet-based de-noising of on-line pd signals captured by Pearson coil in covered-conductor overhead distribution networks. Int J Electr Power Energy Syst 2012;43(1):1185–92. https://doi.org/10.1016/j.ijepes.2012.06.035 http://www.sciencedirect.com/science/article/pii/S0142061512002979 .

[3] Hekmati A. A novel acoustic method of partial discharge allocation considering structure-borne waves. Int J Electr Power Energy Syst 2016;77:250–5. https://doi.org/10.1016/j.ijepes.2015.11.083 http://www.sciencedirect.com/science/article/pii/S0142061515005141 .

[4] Hekmati A. Proposed method of partial discharge allocation with acoustic emission sensors within power transformers. Appl Acoust 2015;100:26–33. https://doi.org/10.1016/j.apacoust.2015.07.011 http://www.sciencedirect.com/science/article/pii/S0003682X15002042 .

[5] Hekmati A, Hekmati R. Optimum acoustic sensor placement for partial discharge allocation in transformers. IET Sci, Meas Technol 2017;11(5):581–9. https://doi.org/10.1049/iet-smt.2016.0417.

[6] Gargari S, Wouters P, van der Wielen P, Steennis E. Statistical approach to identify the discharge source in mv cables and accessories. Condition monitoring and diagnosis, 2008. CMD 2008. International conference on Springer; 2008. p. 1203–6. https://doi.org/10.1109/CMD.2008.4580504.

[7] Gargari S, Wouters P, van der Wielen P, Steennis E. Partial discharge parameters to evaluate the insulation condition of on-line located defects in medium voltage cable networks. IEEE Trans Dielectr Electr Insul 2011;18(3):868–77. https://doi.org/10.1109/TDEI.2011.5931076.

[8] Bowmer C. On-line diagnostic trials on London electricity's 11 kV cable system. In: Asset management of cable systems (Ref. No. 2000/029), IEE seminar on; 2000. p. 7/1–717. https://doi.org/10.1049/ic:20000164.

[9] Aravinthan V, Jewell W. Optimized maintenance scheduling for budget-constrained distribution utility. IEEE Trans Smart Grid 2013;4(4):2328–38. https://doi.org/10.1109/TSG.2013.2271616.

[10] Bangalore P, Tjernberg L. An artificial neural network approach for early fault detection of gearbox bearings. IEEE Trans Smart Grid 2015;6(2):980–7. https://doi.org/10.1109/TSG.2014.2386305.

[11] Behzadirafi S, Salehfar H. Preventive maintenance scheduling based on short circuit and overload currents. IEEE Trans Smart Grid 2015;6(4):1740–7. https://doi.org/10.1109/TSG.2015.2405472.

[12] Russell B, Benner C. Intelligent systems for improved reliability and failure diagnosis in distribution systems. IEEE Trans Smart Grid 2010;1(1):48–56. https://doi.org/10.1109/TSG.2010.2044898.

[13] Wischkaemper J, Benner C, Russell B, Manivannan K. Application of waveform analytics for improved situational awareness of electric distribution feeders. IEEE Trans Smart Grid 2015;6(4):2041–9. https://doi.org/10.1109/TSG.2015.2406757.

[14] Satish L, Gururaj B. Use of hidden Markov models for partial discharge pattern classification. IEEE Trans Electr Insul 1993;28(2):172–82. https://doi.org/10.1109/14.212242.

[15] Salama M, Bartnikas R. Determination of neural-network topology for partial discharge pulse pattern recognition. IEEE Trans Neural Netw 2002;13(2):446–56. https://doi.org/10.1109/72.991430.

[16] Peng X, Zhou C, Hepburn D, Judd M, Siew W. Application of k-means method to pattern recognition in on-line cable partial discharge monitoring. IEEE Trans Dielectr Electr Insul 2013;20(3):754–61. https://doi.org/10.1109/TDEI.2013.6518945.

[17] Niemeyer L. A generalized approach to partial discharge modeling. IEEE Trans Dielectr Electr Insul 1995;2(4):510–28. https://doi.org/10.1109/94.407017.

[18] Noskov M, Malinovski A, Sack M, Schwab A. Modelling of partial discharge development in electrical tree channels. IEEE Trans Dielectr Electr Insul 2003;10(3):425–34. https://doi.org/10.1109/TDEI.2003.1207468.

[19] Van der Wielen P. On-line detection and location of partial discharges in medium-voltage power cables PhD thesis Eindhoven, Netherlands: Eindhoven University; 2005.

[20] Wagenaars P, Wouters P, van der Wielen P, Steennis E. Influence of ring main units and substations on online partial-discharge detection and location in medium-voltage cable networks. IEEE Trans Power Del 2011;26(2):1064–71. https://doi.org/10.1109/TPWRD.2010.2089808.

[21] Wagenaars P. Integration of online partial discharge monitoring and defect location in medium-voltage cable networks PhD thesis Eindhoven, Netherlands: Eindhoven University; 2010.

[22] Veen J. On-line signal analysis of partial discharges in medium-voltage power cables PhD thesis Eindhoven, Netherlands: Eindhoven University; 2005.

[23] Du Z, Mashikian M, Palmieri F. Partial discharge propagation model and location estimate. Electrical insulation, 1994., Conference record of the 1994 IEEE international symposium on 1994. p. 99–102. https://doi.org/10.1109/ELINSL.1994.401458.

[24] Mashikian M. Partial discharge location as a diagnostic tool for power cables. Power engineering society winter meeting, 2000. IEEE, vol. 3. 2000. p. 1604–8. https://doi.org/10.1109/PESW.2000.847582.

[25] Knapp C, Bansal R, Mashikian M, Northrop R. Signal processing techniques for partial discharge site location in shielded cables. IEEE Trans Power Del 1990;5(2):859–65. https://doi.org/10.1109/61.53094.

[26] Steennis EF, Wouters PAA, Van der Wielen PC, Veen J. Method and system for transmitting an information signal over a power cable. US Patent 7,372,280; May 13 2008.

[27] Ma X, Zhou C, Kemp I. Automated wavelet selection and thresholding for PD detection. IEEE Electr Insul Mag 2002;18(2):37–45. https://doi.org/10.1109/57.995398.

[28] Zhou X, Zhou C, Kemp I. An improved methodology for application of wavelet transform to partial discharge measurement denoising. IEEE Trans Dielectr Electr Insul 2005;12(3):586–94. https://doi.org/10.1109/TDEI.2005.1453464.

[29] Zhang H, Blackburn T, Phung B, Sen D. A novel wavelet transform technique for on-line partial discharge measurements. 1. WT de-noising algorithm. IEEE Trans Dielectr Electr Insul 2007;14(1):3–14. https://doi.org/10.1109/TDEI.2007.302864.

[30] Zhang H, Blackburn T, Phung B, Sen D. A novel wavelet transform technique for on-line partial discharge measurements. 2. On-site noise rejection application. IEEE Trans Dielectr Electr Insul 2007;14(1):15–22. https://doi.org/10.1109/TDEI.2007.302865.

[31] Satish L, Nazneen B. Wavelet-based denoising of partial discharge signals buried in excessive noise and interference. IEEE Trans Dielectr Electr Insul 2003;10(2):354–67. https://doi.org/10.1109/TDEI.2003.1194122.

[32] Veen J, van der Wiellen P. The application of matched filters to PD detection and localization. IEEE Electr Insul Mag 2003;19(5):20–6. https://doi.org/10.1109/MEI.2003.1238714.

[33] Wagenaars P, Wouters P, van der Wielen P, Steennis E. Adaptive templates for matched filter bank for continuous online partial discharge monitoring. IEEE Trans Dielectr Electr Insul 2011;18(5):1693–701. https://doi.org/10.1109/TDEI.2011.6032841.

[34] Carrato S, Contin A. Application of a peak detection algorithm for the shape analysis of partial discharge amplitude distributions. Electrical insulation, 1994., Conference record of the 1994 IEEE international symposium on 1994. p. 288–91. https://doi.org/10.1109/ELINSL.1994.401510.

[35] Daubechies I, et al. Ten lectures on wavelets vol. 61. SIAM; 1992.

[36] Powers DM. Evaluation: from precision, recall and f-measure to roc, informedness, markedness and correlation.

[37] Sammut C, Webb GI. Encyclopedia of machine learning. Springer Science & Business Media; 2011.